Normal Modes of Vibration in Nickel

R. J. BIRGENEAU,* J. CORDES,† G. DOLLING, AND A. D. B. WOODS
Chalk River Nuclear Laboratories, Chalk River, Ontario, Canada
(Received 13 July 1964)

The frequency–wave-vector dispersion relation, $\nu(\mathbf{q})$, for the normal vibrations of a nickel single crystal at 296°K has been measured for the [00ζ], [0$\zeta\zeta$], [$\zeta\zeta\zeta$], and [0ζ1] symmetric directions using inelastic neutron scattering. The results can be described in terms of the Born–von Kármán theory of lattice dynamics with interactions out to fourth-nearest neighbors. The shapes of the dispersion curves are very similar to those of copper, the normal mode frequencies in nickel being about 1.24 times the corresponding frequencies in copper. The fourth-neighbor model was used to calculate the frequency distribution function $g(\nu)$ and related thermodynamic properties.

INTRODUCTION

MANY properties of the ferromagnetic transition metal, nickel, have been studied both experimentally and theoretically over the past several years. The electronic band structure and Fermi surface of nickel are believed to be similar in certain respects to those of copper[1,2] whereas the incomplete d-electron shell and ferromagnetic properties of nickel demonstrate its similarity to iron and cobalt.[3] The simple structure (face-centered cubic) and favorable nuclear parameters of nickel make possible, in principle, a study of several of its properties by means of the now well-known[4] techniques of thermal neutron inelastic scattering. Some measurements have already been made[5] of the frequency–wave-vector dispersion relation for long-wavelength spin waves in nickel. The technique of small-angle scattering[6] has also been employed[7] to observe the parabolic form of this dispersion relation. From both types of experiment, values of the nearest-neighbor exchange parameter J have been deduced, which are in good agreement with those obtained from spin-wave resonance[8] experiments and from measurements of the saturation magnetization[9] as a function of temperature. A study has been made[10] of the critical neutron scattering near the Curie temperature (630°K), and of the frequency distribution function for the normal modes of vibration $g(\nu)$.[11–13]

This paper is concerned firstly with the determination of the frequency–wave-vector dispersion relation $\nu_j(\mathbf{q})$ (j is the polarization index) for the normal modes of vibration in a single crystal of unmagnetized nickel at 296°K, by means of *coherent* inelastic neutron scattering,[14] and secondly with the correlation of these results with measurements of other properties of nickel.

In the experiments, coherent one-phonon scattering processes occur in which the energy and momentum of the neutrons are changed from their initial values, E_0 and $\hbar\mathbf{k}_0$ to final values E' and $\hbar\mathbf{k}'$ governed by the conservation conditions:

$$E_0-E'=\pm h\nu, \tag{1}$$

$$\mathbf{k}_0-\mathbf{k}'=\mathbf{Q}=2\pi\boldsymbol{\tau}+\mathbf{q}, \tag{2}$$

where $\mathbf{Q}$ is the momentum transfer vector, $\mathbf{q}$ the reduced wave vector of the phonon involved in the scattering process, and $\boldsymbol{\tau}$ a vector of the reciprocal lattice. The $+$ $(-)$ sign refers to phonon creation (annihilation). Peaks are obtained when the frequency ν given by Eq. (1) coincides with that of the phonon whose wave vector is $\mathbf{q}$, given by the dispersion relation

$$\nu=\nu_j(\mathbf{q}). \tag{3}$$

This process is repeated for successive values of $\mathbf{q}$ along high-symmetry directions in the crystal. Such measurements provide direct information concerning the interatomic forces.

Attempts have been made[15,16] to calculate the interatomic forces in certain metals (e.g., Na, Cu, Zn) from first principles, and to justify[17] the use of an "effective

* Summer visitor, 1963. Present address: Yale University, New Haven, Connecticut.

† Summer visitor, 1963. Present address: Cambridge University, Cambridge, England.

[1] J. C. Phillips, Phys. Rev. **133**, A1020 (1964).

[2] J. Yamashita, M. Fukuchi and S. Wakoh, University of Tokyo, I.S.S.P. Report A75, 1963 (unpublished).

[3] R. M. Bozorth, *Ferromagnetism* (D. Van Nostrand Company, Inc., New York, 1951).

[4] B. N. Brockhouse, *Inelastic Scattering of Neutrons in Solids and Liquids* (International Atomic Energy Agency, Vienna, 1961), p. 113.

[5] K. C. Turberfield, A.E.R.E. (Harwell) Report PR/SSP **4**, 13, 1963 (unpublished).

[6] R. D. Lowde and N. Umakantha, Phys. Rev. Letters, **4**, 452 (1960).

[7] M. W. Stringfellow and B. H. Torrie, A.E.R.E. (Harwell) Report PR/SSP **5**, 18, 1963 (unpublished).

[8] H. Nosé, J. Phys. Soc. Japan **16**, 2475 (1961).

[9] B. E. Argyle, S. H. Charap, and E. W. Pugh, Phys. Rev. **132**, 2051 (1963).

[10] B. Jacrot and D. Cribier, J. Phys. Radium **23**, 494 (1962).

[11] N. A. Tchernoplekov, M. G. Zemlyanov, A. G. Tchetserin, and B. G. Lyashtchenko, *Inelastic Scattering of Neutrons in Solids and Liquids* (International Atomic Energy Agency, Vienna, 1962), Vol. 2, p. 159.

[12] R. M. Brugger, A.E.R.E. (Harwell) Report R 4562, 1964 (unpublished).

[13] B. Mozer, K. Otnes, and H. Palevsky, Phys. Chem. Solids (to be published).

[14] G. Placzek and L. Van Hove, Phys. Rev. **93**, 1207 (1954).

[15] T. Toya, J. Res. Inst. Catalys. Hokkaido University **6**, 183 (1958); also Progr. Theoret. Phys. (Kyoto) **20**, 974 (1958).

[16] W. A. Harrison, Phys. Rev. **129**, 2503 (1963).

[17] W. Cochran, Proc. Roy. Soc. (London) **A276**, 308 (1963).

interatomic potential" to describe these forces. It is hoped that the results contained in this paper will stimulate the further theoretical work required to extend such calculations to the case of transition metals.

When a suitable interatomic force model has been constructed from the observed $\nu_j(\mathbf{q})$, the frequency distribution function $g(\nu)$ for the normal modes may be computed, together with the moments M_n of this function:

$$M_n=\int_0^\infty \nu^n g(\nu)d\nu \Big/ \int_0^\infty g(\nu)d\nu. \qquad (4)$$

These moments may be obtained from a detailed analysis of precise thermodynamic data, such as has been carried out for the alkali halides.[18] This process is, however, more complicated in the case of nickel, since the observed total heat capacity contains contributions from the conduction electrons and from spin waves, in addition to the usual lattice term.

Nickel is one of the few materials for which a comparison is possible between the $g(\nu)$ obtained directly[11] from incoherent neutron scattering experiments and that computed from the normal mode dispersion relation *via* an interatomic force model. A third possible method of determining $g(\nu)$, by means of neutron scattering from a single crystal specimen of natural isotopic composition, and correcting for the coherent scattering effects, has been attempted[12] with some success. Analysis of inelastic neutron scattering from polycrystalline nickel (also of natural isotopic composition) with the help of an "incoherent approximation" has been carried out[13] to obtain a function which is believed to resemble the frequency distribution function of nickel in important respects. A fifth method of obtaining information about $g(\nu)$, recently suggested by Guttman[19] and involving the use of polarized neutron beams, cannot be used in the case of nickel since its incoherent scattering does not arise from nuclear spin disorder.

Similar measurements of $\nu_j(\mathbf{q})$ for nickel by Hautcler[20] have been made independently of those reported in this paper. No detailed comparison of these results has yet been made.

MEASUREMENTS AND RESULTS

The present experiments were performed by means of the triple axis crystal spectrometer[4] at the NRU reactor, Chalk River. A collimated beam of monochromatic neutrons, produced by Bragg reflection from an aluminum single crystal, is incident upon the nickel specimen. The energies of the scattered neutrons are determined by Bragg reflection from a second aluminum single crystal. Most of the experiments consisted in observing the scattered neutron counting rate for fixed values of $\mathbf{Q}$ and E', while the incident energy, $E_0(E_0>E')$ is varied.[4] Measurements were carried out for waves propagating along the high symmetry directions $[00\zeta]$, $[0\zeta\zeta]$, $[\zeta\zeta\zeta]$, and $[0\zeta 1]$.

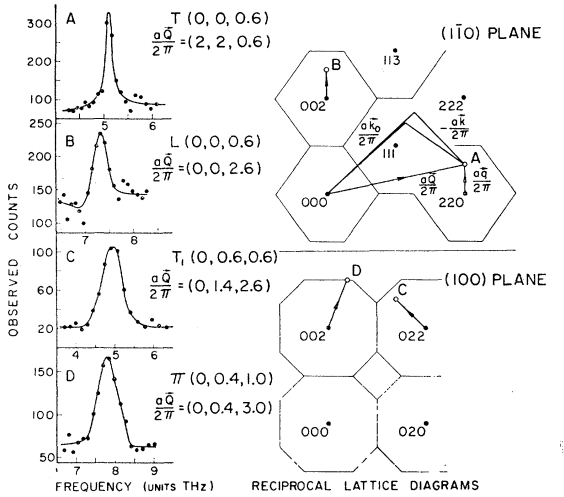

FIG. 1. Neutron groups for typical phonons in nickel and their corresponding positions in the reciprocal lattice (1 THz$=10^{12}$ cps).

The single crystal nickel specimen (purity$\geqslant$99.97%) was in the form of a $\frac{3}{4}$-in.$\times\frac{3}{4}$-in. cylinder, purchased from the Virginia Institute for Scientific Research. Measurements were made at 296°K with the crystal in either of two different orientations (i) with a (1$\bar{1}$0)-type mirror plane parallel to $\mathbf{k}_0$ and $\mathbf{k}'$, or (ii) with a (100)-type mirror plane parallel to $\mathbf{k}_0$ and $\mathbf{k}'$. Certain branches of $\nu_j(\mathbf{q})$, such as the longitudinal (L) and transverse (T) branches in the $[00\zeta]$ direction may be studied in both crystal orientations; this serves as a useful consistency check on the results, as do observations of the same phonon for different $\mathbf{Q}$ and for different E'. The experimental arrangement is such that the instrumental resolution is generally speaking higher for low E'. In the experiments at low E', care was taken to avoid the possibility of spurious neutron groups arising from the second-order reflecting power of the analyzing crystal, thus:

$$E_0-4E'=\pm h\nu',$$
$$\mathbf{k}_0-2\mathbf{k}'=\mathbf{Q}'=2\pi\boldsymbol{\tau}+\mathbf{q}', \qquad (5)$$

where $\nu'=\nu_j(\mathbf{q}')$. Other types of spurious processes can also occur, though these are usually more readily avoided.

Four typical neutron groups are shown in Fig. 1; groups A and B were observed under conditions of higher resolution than C and D, as is suggested by their relative frequency widths. The upper reciprocal lattice diagram in Fig. 1 contains a graphical representation of Eq. (2) and illustrates the method of "constant $\mathbf{Q}$."[4] The neutron group A was obtained by

[18] T. H. K. Barron, W. T. Berg, and J. A. Morrison, Proc. Roy. Soc. (London) **A242**, 478 (1957).
[19] L. Guttman, Nucl. Instr. Methods **25**, 188 (1963).
[20] S. Hautcler (private communication).

observing the scattered neutron count rate for a sequence of spectrometer positions, the first and last of which are indicated by means of the appropriate neutron wave vectors. The complete results are shown in Fig. 2 and Table I. The phonon frequencies were

TABLE I. Normal mode frequencies in nickel at 296°K (units THz≡10^{12} cps).

$[00\zeta]L$		$[00\zeta]T$		$[\zeta\zeta\zeta]L$	
ζ	ν	ζ	ν	ζ	ν
0.1	1.71±0.10	0.2	2.03±0.04	0.1	3.05±0.05
0.2	3.12±0.09	0.3	2.99±0.06	0.15	4.39±0.07
0.3	4.42±0.11	0.4	3.83±0.06	0.2	5.60±0.09
0.4	5.58±0.12	0.5	4.49±0.08	0.25	6.61±0.10
0.5	6.54±0.13	0.6	5.12±0.09	0.3	7.44±0.14
0.6	7.34±0.12	0.7	5.67±0.11	0.35	8.14±0.16
0.7	7.94±0.14	0.75	5.83±0.12	0.4	8.53±0.17
0.8	8.34±0.13	0.8	6.01±0.12	0.425	8.61±0.24
0.85	8.50±0.24	0.85	6.07±0.12	0.45	8.79±0.18
0.9	8.56±0.18	0.9	6.23±0.13	0.475	8.58±0.25
0.95	8.65±0.20	0.95	6.24±0.14	0.5	8.88±0.17
1.0	8.55±0.13	1.0	6.27±0.10		
$[\zeta\zeta\zeta]T$		$[0\zeta\zeta]L$		$[0\zeta\zeta]T_2$[a]	
ζ	ν	ζ	ν	ζ	ν
0.1	1.33±0.04	0.1	2.34±0.09	0.1	1.28±0.05
0.15	1.89±0.05	0.2	4.44±0.11	0.2	2.76±0.10
0.2	2.47±0.05	0.3	6.08±0.10	0.3	4.14±0.14
0.25	2.99±0.05	0.4	7.25±0.17	0.4	5.50±0.18
0.3	3.37±0.05	0.5	7.63±0.20	0.5	6.15±0.12
0.35	3.76±0.05	0.55	7.69±0.27	0.6	6.85±0.20
0.375	3.90±0.07	0.6	7.68±0.18	0.65	7.22±0.18
0.4	4.02±0.06	0.65	7.47±0.19	0.7	7.67±0.15
0.425	4.10±0.08	0.7	7.39±0.17	0.75	7.93±0.23
0.45	4.26±0.06	0.75	7.30±0.24	0.8	8.13±0.14
0.475	4.24±0.08	0.8	6.85±0.17	0.9	8.52±0.17
0.5	4.24±0.06	0.85	6.74±0.25		
		0.9	6.54±0.17		
		0.95	6.36±0.15		
$[0\zeta\zeta]T_1$[a]		$[0\zeta 1]\Lambda$		$[0\zeta 1]\Pi$	
ζ	ν	ζ	ν	ζ	ν
0.2	1.96±0.05	0.5	6.21±0.15	0.1	8.52±0.20
0.3	2.81±0.08	0.6	6.20±0.12	0.2	8.39±0.15
0.4	3.62±0.09	0.7	6.40±0.14	0.3	8.16±0.16
0.5	4.36±0.08	0.8	6.36±0.15	0.4	7.83±0.14
0.6	4.98±0.10	0.9	6.32±0.16	0.5	7.49±0.14
0.7	5.59±0.12			0.6	7.11±0.13
0.8	5.97±0.13			0.7	6.80±0.12
0.9	6.26±0.15			0.8	6.47±0.12
				0.9	6.40±0.11

[a] The polarization vectors for the T_1 and T_2 modes propagating along the $[0\zeta\zeta]$ direction are parallel to $[0\bar{\zeta}\zeta]$ and $[\zeta 00]$, respectively.

determined with a precision of about 2%. They have been corrected for the effect of the variation of the neutron scattering cross section across the instrumental energy resolution. The solid lines drawn through the origin ($q=0$) in various sections of Fig. 2 represent the appropriate sound velocities calculated from the elastic constants of unmagnetized nickel.[21] The apparent discrepancies between these lines and the phonon frequencies measured at small wave vectors for the $L[00\zeta]$ and $T_2[0\zeta\zeta]$ branches are probably within

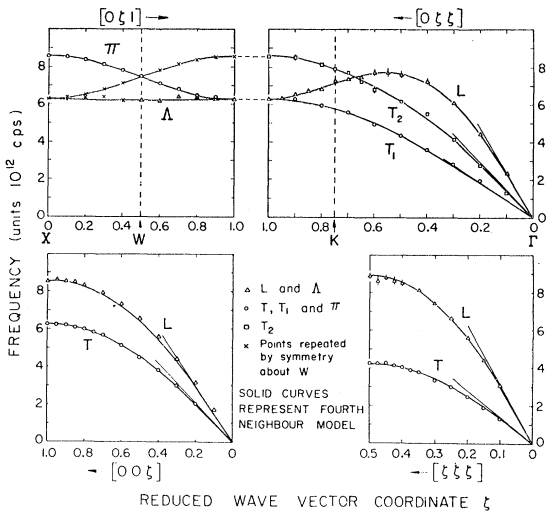

FIG. 2. The measured dispersion curves for nickel at 296°K compared with the best-fit fourth-neighbor Born–von Kármán model. The straight lines through the origins have the slopes of the appropriate velocities of sound as calculated from the measured elastic constants.

experimental error. (The polarization vectors of the normal modes belonging to the $T_2[0\zeta\zeta]$ branch are parallel to $[\zeta 00]$.) More precise measurements would be needed to establish the significance of these discrepancies. The dispersion curves are generally rather smooth and do not display anomalies of the type observed, for example, in the case of lead.[22]

In the present experiments, no observations were made of neutron groups arising from "one-magnon" scattering processes (i.e., involving one quantum of spin-wave energy). It is easy to avoid any confusion between phonon and magnon processes owing to the large energy difference between them for most wave vectors. Figure 3 shows a sketch of the magnon dispersion relation (as a function of the square of the wave vector) expected from simple spin-wave theories of ferromagnetism[23,5,7]; the upper shaded area is a rough indication of the uncertainty of the dashed curve. Although such theories are adequate for perhaps only the region of small wave vectors, it seems very unlikely that the actual magnon energies for large wave vectors are within the "phonon" energy region, represented by the lower shaded portion. For small wave vectors, in this method of presentation, the magnon dispersion relation is a linear function with a very small or zero intercept at $q^2=0$. The phonon dispersion curves, on the other hand, appear parabolic near the origin, and will thus intersect the magnon curve. These intersections will occur for $aq/2\pi \lesssim 0.1$ in all cases. [The reverse situation, in which the magnon curves are being

[21] J. de Klerk, Proc. Phys. Soc. (London) **73**, 337 (1959).

[22] B. N. Brockhouse, T. Arase, G. Caglioti, K. R. Rao, and A. D. B. Woods, Phys. Rev. **128**, 1099 (1962).

[23] J. Van Kranendonk and J. H. Van Vleck, Rev. Mod. Phys. **30**, 1 (1958).

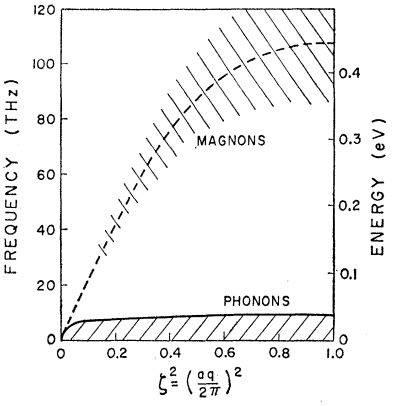

FIG. 3. Comparison of phonon and magnon energies for nickel.

studied, and the phonons avoided, would be much less favorable; it would be necessary to distinguish, by means of the response of the neutron intensity to an applied magnetic field, the true magnon peaks from various one-phonon processes (for which the cross section would usually be much higher) observed by reason of the higher order reflections from the monochromator and analyzer crystals of the spectrometer. A study of the phonon dispersion relation is thus a valuable preliminary for the more difficult determination of the spin-wave dispersion relation.]

ANALYSIS OF RESULTS

The application of the Born–von Kármán theory[24] to fcc lattices has been described by many authors. The squares of the normal mode frequencies are eigenvalues of a 3×3 matrix **D** whose elements have been expressed in a concise form by Squires.[25] For normal modes propagating in the high-symmetry directions (see Fig. 2), **D** factorizes into three linear equations. The dispersion curves can then be Fourier analyzed[26] to yield information concerning the forces between various planes of atoms in the crystal. This kind of analysis is described in detail in Ref. 22 for the case of lead. As might be expected from the smooth shapes of the dispersion curves for nickel, Fourier analysis shows that relatively short range interatomic forces (at least up to third-nearest neighbors, but not necessarily beyond fifth) provide a satisfactory description of the experimental results. This is confirmed by a linear least-squares fit analysis of all the data of Table I together with the known elastic constants,[21] on the basis of the Born–von Kármán theory. An excellent fit was obtained either with general interatomic forces out to fourth-nearest neighbors, or with an axially symmetric model[27] extending to fifth-nearest neighbors. The dispersion curves are indeed sufficiently simple that a fairly satisfactory fit can be obtained with a third-neighbor force model having only 9 disposable parameters. The dispersion curves calculated on the basis of the general fourth-neighbor model are shown in Fig. 2. The force constant notation used, and their least-squares fitted values for both the general fourth-neighbor model and axially symmetric fifth-neighbor model, are given in Table II. Some properties of nickel utilized in the analysis are listed in Table III. Certain low-frequency modes and elastic constants are not very well fitted by the model, although this lack of fit is probably not significant. It is possible that the elastic constant measurements[21,28] are sensitive to small amounts of impurity or varying heat treatments, and therefore may not correspond exactly to those appropriate to the present specimen. Furthermore, no special efforts were made in the present experiments to make high precision measurements of $\nu(\mathbf{q})$ for low $\mathbf{q}$.

The fourth neighbor force model described in Table

TABLE II. Force constant notation and best fit values.

Neighbor location	Force constants			Values (dyn/cm) (a) General forces	(b) Axially symmetric forces
First (1, 1, 0)	α_1	γ_1	0	$\alpha_1=17\,178$	$\alpha_1=17\,720$
	γ_1	α_1	0	$\beta_1=-26$	$\beta_1=-1015$
	0	0	β_1	$\gamma_1=19\,316$	$\gamma_1=\alpha_1-\beta_1$
Second (2, 0, 0)	α_2	0	0	$\alpha_2=880$	$\alpha_2=1148$
	0	β_2	0	$\beta_2=-519$	$\beta_2=-998$
	0	0	β_2		
Third (2, 1, 1)	α_3	γ_3	γ_3	$\alpha_3=626$	$\alpha_3=940$
	γ_3	β_3	δ_3	$\beta_3=320$	$\beta_3=182$
	γ_3	δ_3	β_3	$\gamma_3=453$	$\gamma_3=2(\alpha_3-\beta_3)/3$
				$\delta_3=-173$	$\delta_3=(\alpha_3-\beta_3)/3$
Fourth (2, 2, 0)	α_4	γ_4	0	$\alpha_4=275$	$\alpha_4=459$
	γ_4	α_4	0	$\beta_4=-160$	$\beta_4=-153$
	0	0	β_4	$\gamma_4=424$	$\gamma_4=\alpha_4-\beta_4$
Fifth[a] (3, 1, 0)	α_5	δ_5	0		$\alpha_5=-363$
	δ_5	β_5	0		$\beta_5=100$
	0	0	γ_5		$\gamma_5=(9\beta_5-\alpha_5)/8$
					$\delta_5=3(\alpha_5-\beta_5)/8$

[a] There is insufficient data for an analysis in terms of a general fifth-neighbor model.

TABLE III. Some properties of nickel at 296°K.

Mass = 58.71 amu
Lattice constant = 3.5239 Å
Elastic constants[a] (units 10^{12} dyn/cm^2):
$C_{11}=2.46$, $C_{12}=1.50$, $C_{44}=1.22$

[a] The precision of the elastic constant values is believed to be better than 1%.

[24] M. Born and K. Huang, *Dynamical Theory of Crystal Lattices* (Clarendon Press, Oxford, England, 1954).
[25] G. L. Squires, Arkiv Fysik **25**, 21 (1963).
[26] A. J. E. Foreman and W. M. Lomer, Proc. Phys. Soc. (London) **B70**, 1143 (1957).
[27] G. W. Lehman, T. Wolfram, and R. E. De Wames, Phys. Rev. **128**, 1593 (1962).
[28] G. A. Alers, J. R. Neighbours, and H. Sato, Bull. Am. Phys. Soc. 4, 131 (1959).

II has been used as an interpolation formula to compute the frequencies of normal modes which have not been directly observed in the present experiments. All the frequencies thus calculated were found to have plausible values. It seems reasonable, therefore, that the frequency distribution function $g(\nu)$ for the normal modes may be calculated to a good approximation with the help of this model. The problem of obtaining $g(\nu)$ from the observed $\nu_j(\mathbf{q})$ or from derived force models has been widely studied; the various possible methods have been summarized by Maradudin *et al.*[29] It has recently been emphasized[30] that all thermodynamic data may be derived from the moments M_n of $g(\nu)$, defined by Eq. (4), and that it is therefore unnecessary to compute $g(\nu)$ itself for the purposes of thermodynamics. The most common objection raised against the direct computation of $g(\nu)$ from a force model by the sampling method[29] is that the size of the sample required to correctly reproduce singular features of $g(\nu)$, such as critical points, is much too large for calculation even on high speed electronic computers. This difficulty has been largely overcome by means of a new sampling method developed by Gilat and Dolling[31] in which the *effective* sample size is enormously increased with very little increase in computing time. Details of the actual calculation of $g(\nu)$ for nickel using this method are given in Appendix A. The resulting distribution function is shown as the solid line in Fig. 4; the principal critical points[32] are very clearly displayed, and may be correlated with the appropriate points on the dispersion curves (Fig. 2). The solid line is in fact a histogram plot with steps in frequency of 0.02 THz (1 THz$=10^{12}$ cps) but the spacing and fluctuation of the individual blocks are too small to be plotted separately. Special attention has been devoted (see Appendix A) to maintain high accuracy in the relatively unpopulated region of low frequencies. The dashed curve in Fig. 4 shows the results of Tchernoplekov *et al.*[11] obtained from measurements of incoherent inelastic neutron scattering from a sample of nickel isotopes for which the coherent cross section was zero. These results are plotted on an arbitrary vertical scale, since it is not possible to normalize them correctly with respect to the area under the computed curve. The experimental errors are rather large, particularly for $\nu<1$ or <9 THz, and the critical points are not clearly shown. There is, however, qualitative agreement between the measured and calculated curves. The solid circles represent the results of Brugger[12] obtained from observations of the total inelastic scattering from a single crystal of ordinary nickel as a function of crystal orientation. The energy resolution was insufficient to show the narrow peak near $\nu=8$ THz.

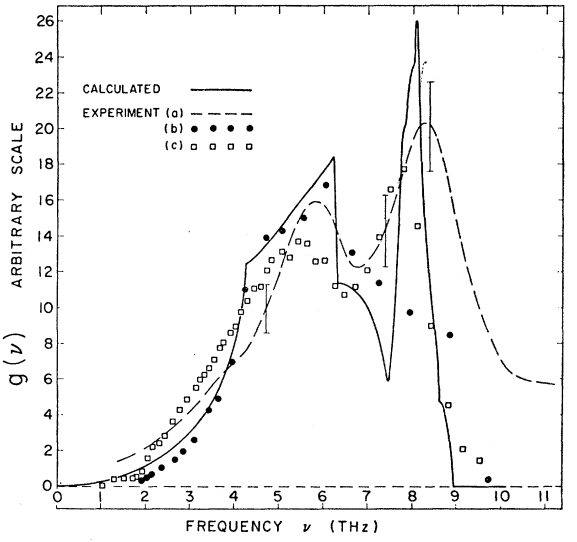

FIG. 4. Frequency distribution function of nickel determined by various methods as described in the text. The experimental results (a), (b), and (c) are taken from Refs. 11, 12, and 13, respectively.

At lower frequencies, the resolution was somewhat better, and the agreement with the computed curve is quite good. The analysis performed by Mozer *et al.*,[13] mentioned in the Introduction, is represented by the open squares. Both these results and those of Brugger have been normalized to the area under the computed curve. In view of the crude assumptions employed in Ref. 13 to extract $g(\nu)$ from the experimental observations, the agreement between the square points and solid curve is remarkably good. Experimental measurements of $g(\nu)$ with much higher energy resolution are, however, needed in order to provide an adequate test of the computed distribution function of Fig. 4.

The departure of the distribution function from that expected on the basis of the Debye theory is well illustrated by a plot of $g(\nu)/\nu^2$, as shown in Fig. 5. The intercept at $\nu=0$ corresponds to a Debye "cutoff" frequency ν_c of 9.374 THz, from which we obtain θ_D (at 0°K)$=h\nu_c/k_B=449.9$°K. (k_B is Boltzmann's constant.) An expansion of the low-frequency part of $g(\nu)$ in even powers of ν

$$g(\nu)=a_2\nu^2+a_4\nu^4+a_6\nu^6+\cdots, \tag{6}$$

showed that a_4, a_6, etc., were negligible for ν up to about 0.9 THz. The most usual way to present results of $g(\nu)$ computations for comparison with thermodynamic properties is to evaluate θ_D as a function of temperature. This function is shown in Fig. 6(a). It should be emphasized that this curve has been computed essentially from dispersion curves measured only at room temperature. No attempt has been made to correct the various derived functions (θ_D, M_n) for anharmonic effects which introduce a slight temperature dependence (a few percent for temperatures less than

[29] A. A. Maradudin, E. W. Montroll, and G. H. Weiss, *Solid State Physics*, edited by F. Seitz and D. Turnbull (Academic Press Inc., New York, 1963), Suppl. 3.
[30] C. Isenberg, Phys. Rev. 132, 2427 (1963).
[31] G. Gilat and G. Dolling, Phys. Letters 8, 304 (1964).
[32] L. Van Hove, Phys. Rev. 89, 1189 (1953).

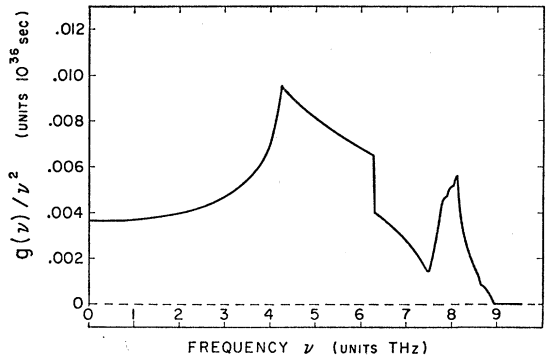

FIG. 5. Calculated $g(\nu)/\nu^2$ for nickel at 296°K.

296°K) of the normal mode frequencies. We therefore expect the computed θ_D to be about 10°K too low at very low temperatures.

Also shown in Fig. 6(a) is a curve representing the experimental heat capacity data of Busey and Giauque[33] and of Rayne and Kemp,[34] as interpreted by the latter authors. As mentioned in the Introduction, the analysis of heat capacity (C_v) data for nickel is complicated by the existence of a magnetic contribution C^m, in addition to the usual conduction electron (C^e) and lattice (C^l) terms. Thus an analysis of $C_v(T)$ for $T<10$°K by means of the formula

$$C_v=C^e+C^l=\gamma T+\beta T^3 \tag{7}$$

is quite inadequate in the case of nickel. In the absence of a magnetic field, the dominant term[35] in C^m is of the form $AT^{3/2}$ for low T. The existing C_v data for nickel are not sufficiently precise to determine the value of A. This can be found, however, from saturation magnetization measurements, and the appropriate allowance for C^m made in the analysis of C_v. In this way, Rayne and Kemp[34] have deduced the "experimental" curve shown in Fig. 6(a). At 0°K, they obtain $\theta_D=468$°K. (A somewhat more accurate estimate of C^m, using a better value[7,9] for the coefficient A, and making allowance for the nonzero intrinsic field in nickel, shows that C_m and therefore also θ_D is rather less than that estimated in Ref. 34.) If no allowance is made for the magnetic contribution, Rayne and Kemp obtain θ_D (0°K)=441°K. The difficulties of estimating θ_D from low-temperature calorimetric data are illustrated by the wide variety of values in the literature.[36] It is clear, however, that very accurate calorimetric data for nickel over a wide temperature range would provide a most valuable check on theoretical calculations of the various contributions to the total heat capacity.

Estimates of θ_D (0°K) may also be made from the elastic constants measured at very low temperatures. Alers *et al.*[28] have obtained $\theta_D=476$°K for nickel under conditions of saturation induction. The value appropriate to unmagnetized nickel is probably somewhat lower than this, if the room temperature results of de Klerk[21] are taken as a guide.

Taking the above considerations into account, the agreement between the two curves in Fig. 6(a) may be regarded as quite satisfactory; it provides additional support for the validity of the Born–von Kármán force model constructed from the observed $\nu_j(\mathbf{q})$ results.

An instructive way[18] to express the frequency-distribution result, which is more generally useful for the purpose of comparison with calorimetric data, is by means of its moments M_n, defined by Eq. (4). These, in turn, can be conveniently expressed in terms of "Debye frequencies," ν_n, defined for $n>-3$ by

$$\nu_n=[(n+3)M_n/3]^{1/n} \quad \text{for} \quad n\neq 0. \tag{8}$$

It can also be shown that

$$\nu_{-3}=(k_B/h)\theta_D(0\text{°K})$$

and

$$\nu_0=\exp\left\{\frac{1}{3}+\int_0^\infty g(\nu)\ln\nu d\nu \Big/ \int_0^\infty g(\nu)d\nu\right\}.$$

The variation of ν_n with n, computed from the distribution function, which in turn was derived from the measured dispersion relation, is shown in Fig. 6(b). (In the simple Debye theory, ν_n is of course a constant, the "cutoff" frequency.) The existing heat capacity data for nickel have not been analyzed so as to extract ν_n values for comparison with this calculated curve.

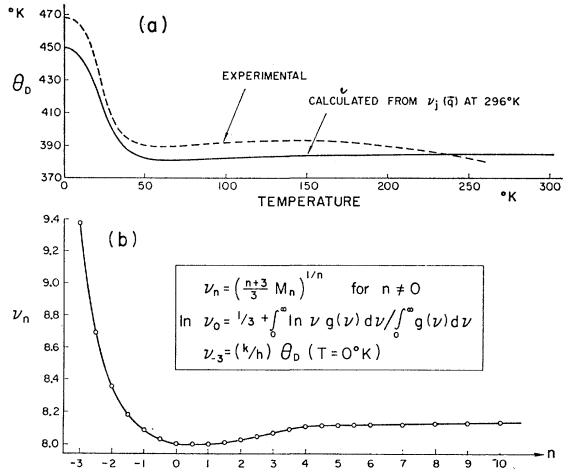

FIG. 6. (a) Comparison of calculated and experimental values of the Debye temperature. (b) Calculated "Debye frequencies," ν_n.

[33] R. H. Busey and W. F. Giauque, J. Am. Chem. Soc. **74**, 3157 (1952).
[34] J. A. Rayne and W. R. G. Kemp, Phil. Mag. **1**, 918 (1956).
[35] F. J. Dyson, Phys. Rev. **102**, 1217 (1956).
[36] W. H. Keesom and C. W. Clark, Physica **2**, 513 (1935); J. C. Walling and P. B. Bunn, Proc. Phys. Soc. (London) **74**, 417 (1959); K. P. Gupta, C. H. Cheng, and P. A. Beck, Phys. Chem. Solids **25**, 73 (1964). The θ_D values given in these references are 413, 348, and 330°K, respectively.

DISCUSSION

The main features of the dispersion relation for normal modes propagating in the principal symmetry directions in nickel at 296°K have been determined. It is of interest to compare these results with the dispersion relation found[37,38] for copper. Cribier *et al.*[37] have measured $\nu_j(\mathbf{q})$ for the $[00\zeta]$, $[0\zeta\zeta]$, and $[\zeta\zeta\zeta]$ directions. Preliminary results of Sinha and Squires[38] for the first two directions are in agreement (within the experimental errors of about 5%) with the earlier results. The available data are barely sufficient to perform a detailed analysis as described above for nickel. Sinha and Squires have attempted, with fair success, to fit their results by means of a modified form of the model proposed by Toya.[15] Both the experimental and theoretical dispersion curves for copper show a striking similarity to those obtained for nickel. The phonon frequencies in copper, apart from certain L modes very close to the $[0\zeta\zeta]$ zone boundary, are on the average a factor 1.24 less than the analogous frequencies in nickel. The individual ratios are the same within experimental error, though there is a tendency for slightly higher ratios to be associated with the lower frequencies and vice versa. The exceptional $L[0\zeta\zeta]$ modes are in any case not well fitted by the model of Sinha and Squires (which fits the simple ratio rule quite closely). The elastic constants C_{11} and C_{44} and the values of θ_D ($T=0$°K) are also consistent with the rule, but the ratio appropriate to C_{12} is about 10% too low. An analysis of heat capacity data to obtain the "Debye frequencies" ν_n has not yet been carried out for nickel. Values of ν_n for copper have, however, been deduced[39] for $n=-3, -2, -1, +2, +4$ and $+6$. The ratios of the ν_n *calculated* for nickel to the *observed* values for copper are 1.30, 1.25, 1.23, 1.21, 1.21, and 1.22, respectively. Perhaps this correlation between copper and nickel, crude and unsophisticated though it may be, is an indication that the normal modes of vibration in nickel may be adequately treated within the theoretical framework developed by Toya[15] and Cochran.[17] Finally, we emphasize the need for more extensive and precise calorimetric data for nickel and neutron scattering data for copper, in order to facilitate the achievement of detailed and comprehensive explanations of the thermal, magnetic and electronic properties of these two metals.

[37] D. Cribier, B. Jacrot and D. Saint-James, Ref. 3, p. 549.
[38] S. Sinha and G. L. Squires, Phys. Chem. Solids (to be published).
[39] L. Salter and J. A. Morrison (private communication).

APPENDIX A

The irreducible 1/48 of the Brillouin zone (BZ) is taken to be defined by the five planes $aq_x/2\pi=1$, $q_z=0$, $q_y=q_z$, $q_x=q_y$, and $(q_x+q_y+q_z)a/2\pi=1.5$. This polyhedron is subdivided into three parts labeled A, B, C in order of increasing q_x values, by the planes $aq_x/2\pi=0.125$ and $aq_x/2\pi=0.0625$. The normal mode frequencies are computed for wave vectors lying on a simple cubic mesh (CM) of spacing $aq/2\pi=1/144$. CM is chosen so that the origin Γ (and, in fact, all the corner points of BZ) of reciprocal space lies at the body center of a basic cube of the mesh. This choice is substantially more efficient than the other alternative, in which Γ lies at a corner point of the mesh. A straightforward calculation of $g(\nu)$ on this basis would involve 254 040 matrix diagonalizations to obtain a total of 35 831 808 phonon frequencies in the entire zone. This difficulty is avoided by diagonalizing the matrix **D** at points throughout the region C (high $\mathbf{q}$) on a "crude" mesh of spacing $aq/2\pi=1/16$. At each $\mathbf{q}$ value (labeled X, say) the frequency gradients $\partial\nu_j/\partial q_i$ are computed by simple perturbation theory; the phonon frequencies corresponding to the 729 points of the basic mesh CM, which lie in the vicinity of each X, are then computed by straightforward linear extrapolation. This method may not be sufficiently accurate[31] over the whole of BZ, particularly at small wave vectors. Thus we diagonalize the matrix **D** for wave vectors on an "intermediate" mesh of spacing $aq/2\pi=1/48$ over the region B, and utilize perturbation theory at each point to compute only nine basic mesh points CM. Finally, the region C of the zone ($aq_x/2\pi<0.0625$) is treated by diagonalization at all CM points, without the use of perturbation theory. The distribution function $g(\nu)$ thus calculated (see Fig. 4) is believed to be an extremely accurate representation of the general fourth-nearest-neighbor force model (Table II). It is adequate for the computation of all thermodynamic quantities except those which are sensitive to the moments M_n of $g(\nu)$ for $n\leqslant -2$. In order to increase the accuracy of $g(\nu)$ for very low frequencies, a second calculation was made for the regions A and B (i.e., for $aq_x/2\pi<0.125$) of BZ. The spacing of the basic mesh CM was $aq/2\pi=1/720$, five times smaller than in the first calculation. A three-stage system of computation was again employed, and the results of the two calculations added together after proper normalization. The results shown in Figs. 4, 5, and 6 are based on this "combined" $g(\nu)$. All these computations were performed on the Control Data G-20 computer at Chalk River; the total computing time involved in producing the data for Figs. 4, 5, and 6 was about 25 min.